PERGAMON

International Journal of Heat and Mass Transfer 42 (1999) 2233–2242

International Journal of HEAT and MASS TRANSFER

Ice and water film growth from incoming supercooled droplets

T.G. Myers[a,*], D.W. Hammond[b]

[a] *Applied Mathematics and Computing Group, Cranfield University, Cranfield, Bedfordshire MK43 0AL, U.K.*
[b] *BAe Sowerby Research Centre, Department 256, FPC 677, PO Box 5, Bristol BS12 7QW, U.K.*

Received 16 April 1998; in final form 24 July 1998

Abstract

A one-dimensional model for ice growth in the presence of an incoming supercooled fluid is developed by specifying a Stefan problem. A number of assumptions are made, relevant to relatively thin ice and water layers, which allow the thermal problem to be solved exactly in terms of the layer thicknesses and ambient conditions. The ice thickness is then determined by combining the mass balance with the phase change condition to reduce the problem to a single first-order ordinary differential equation, which requires a numerical solution. Quantities such as the water film thickness and temperature profiles in the ice and water can be determined easily once the ice thickness is known. Results are presented showing ice and water growth, subject to various ambient conditions. Qualitative agreement with experiment is also shown and the implications of the results to the physical process discussed.

Nomenclature

a_0 energy source terms ($= (r\bar{H}_{aw}W^2/2c_a+\beta W^3G/2)/\kappa_w$) [K m^{-1}]
a_1 energy sink terms ($= (\bar{H}_{aw}+\beta WGc_w+\chi e_0)/\kappa_w$) [m^{-1}]
a_2 coefficient for conduction through ice ($= \kappa_i(T_f-T_s)/\rho_iL$) [m^2 s^{-1}]
a_3 coefficient for conduction through water ($= \kappa_w(a_0-a_1(T_f-T_a))/\rho_iL$) [m s^{-1}]
a_4 measure of heat transfer between ice and substrate ($= \kappa_i/\bar{H}_{is}$) [m]
$B(t)$ ice layer thickness [m]
c specific heat [J kg^{-1} K^{-1}]
e saturation vapour pressure (temperature dependent) [Pa]
e_0 vapour pressure constant (see [8]) [Pa K^{-1}]
G liquid water content [kg m^{-3}]
$h(t)$ water layer thickness [m]
$\bar{H}_{xy}$ heat transfer coefficient between components x and y [W m^{-2} K^{-1}]
l_e Lewis number
L latent heat of fusion [J kg^{-1}]
L_E latent heat of evaporation [J kg^{-1}]
L_s latent heat of sublimation [J kg^{-1}]
p_0 ambient pressure [Pa]
r local recovery factor
T ice temperature [K]
W free stream velocity [m s^{-1}].

Greek symbols

β collection efficiency
θ water temperature [K]
κ thermal conductivity [W m^{-1} K^{-1}]
ρ density [kg m^{-3}]
χ evaporation coefficient, $0.622\bar{H}_{as}L_E/c_ap_0l_e^{2/3}$ (see [1, 2]) [m s^{-1}]
χ_s sublimation coefficient, $0.622\bar{H}_{as}L_s/c_ap_0l_e^{2/3}$ (see [1, 2]) [m s^{-1}].

Subscripts

a air
d droplets

* Corresponding author. Tel.: 00 44 1234 750 111; fax: 00 44 1234 750 728; e-mail: t.g.myers@cranfield.ac.uk

0017-9310/99/$ - see front matter
PII: S0017-9310(98)00237-3

i ice
s substrate
w water.

1. Introduction

Atmospheric clouds of liquid water droplets frequently extend to altitudes at which the droplets become super-cooled. Depending on the nature of the cloud condensation nuclei, freezing may not occur until the droplets become super-cooled down to -40°C. If an aircraft encounters such a cloud, the droplets which strike the surface are provided with a nucleation site and so begin to freeze, giving rise to ice accretions which may rapidly degrade the aerodynamic performance.

In order to satisfy demands for safe flight in all but extreme weather conditions, nearly all commercial aircraft and some helicopters are provided with ice protection systems. A typical system for a long-range passenger jet consumes of the order of 10^5 W when active. This power requirement (as hot air) must be available in all phases of flight and requires significant compromises in the design of the engine. As wing design develops and improvements are made in engine efficiency, it becomes all the more important not to discard the benefits of these technological improvements by fitting an overburdensome or ineffective ice protection system.

Ice prediction models have already had a major impact on the design of aircraft and have helped cut development times and costs significantly. They can also help control the risks of flight testing a new aircraft in icing conditions (see [3] for a review of ice accretion and protection methods). Codes such as LEWICE, TRAJICE 2 and ONERA function well in very cold conditions when rime ice forms (typically below -10°C, when all of the water droplets freeze almost instantaneously and consequently remain in the vicinity of where they strike the aircraft). In mild freezing conditions however, the water may not completely freeze near the impact point but can run back and form pronounced ridges of glaze ice. The existing codes will predict glaze ice shapes via an energy balance, but these predictions may be inaccurate and so need to be checked on an aircraft by aircraft basis.

The work described in this paper forms part of the ICECREMO project, to develop a three-dimensional aircraft icing code (see Acknowledgement). The present investigation is concerned with a one-dimensional model which accounts for the freezing and water build-up, using a Stefan or phase change approach. Already, work has been carried out on the flow of a thin film of water on a fast moving surface [4, 5]. The one-dimensional model is viewed as an appropriate starting place for two reasons. Firstly, the relatively simple system means the results are easier to interpret and the role played by each mechanism driving the ice growth can be identified. Secondly, the ice accretions of interest in this work are typically a few millimetres thick, the radius of curvature of an aerofoil will be considerably greater, $O(0.5\,\mathrm{m})$ on a fixed wing aircraft, so the ice perceives a nominally flat surface. Provided the local conditions, such as droplet catch efficiency and shear stress vary on the length-scale of the curvature and not the ice thickness, the problem can be adequately approximated as one-dimensional. Future work will extend to two and three dimensions and combine the water flow model with the present ice growth work, to provide more accurate predictions of ice shapes and also give information on the development of the microstructure of the ice.

Although the main motivation for this work is aircraft ice accretion, the results and techniques have a wide range of practical applications. Stefan problems are frequently used to describe melting or solidification, for example in the casting of steel or lava flows (see [6, Chap. 1, 7]). Ice accretion is important not only in the aircraft industry, but also for marine engineers and manufacturers of power cables. In fact, the present work is closely related to that of Poots [2, 8], which concerns ice growth on overhead power lines, with two major differences. The first lies in the energy terms, clearly different terms will dominate on a fast moving aircraft and a stationary power cable (unless the wind speed is considerable!). The second, and main difference, is that the earlier work neglects the water thickness when calculating the temperature in the water layer. The Stefan condition then reduces to a form that is immediately integrable. The following work indicates that neglecting this film thickness significantly affects the results, provided the temperature difference between the water surface and the air is $O(1)$. The resultant Stefan condition then requires solving numerically.

In the following section, the standard method employed in most aircraft icing codes, based on an energy argument, is described. The one-dimensional Stefan problem will then be specified and subsequently simplified, exploiting the thinness of the layers to determine the leading order problem. Results for the ice and water layer thicknesses under various ambient conditions are then presented and shown to agree qualitatively with experimental work. The implication of these results to real ice accretions is also discussed.

2. Mathematical formulation

2.1. Messinger model

The basic mathematical formulation is described by the one-dimensional Stefan or phase change problem. This involves solving the heat equations in both the ice and water, coupled with a Stefan condition at the moving

phase change boundary. However, a more popular approach, employed by engineers and the aerospace industry is to tackle the problem via an energy balance. This approach is based on the work of Messinger [9]. The balance relies on equating the heat lost from the ice/water system to the air or substrate (see Fig. 1). The mechanisms for losing energy are:

- Convective heat transfer at the water surface, $Q_c = \bar{H}_{aw}(T_w - T_a)$
- Evaporative heat loss, $Q_e = \chi(e(T_w) - e(T_a))$
- Cooling by incoming droplets, $Q_d = \beta WGc_w(T_w - T_d)$.

Those for gaining energy are:

- Kinetic energy of incoming droplets, $Q_k = (\beta WG)W^2/2$
- Release of latent heat, $Q_l = \rho L\, \partial B/\partial t$
- Aerodynamic heating, $Q_a = r\bar{H}_{aw}W^2/2c_a$.

Conduction through the ice may remove or add heat

- $Q_f = \kappa_i\, \partial T/\partial z$.

Water flow will also affect the heat balance, although this will not be considered in the present one-dimensional model. Provided the water temperature is not too different from that of the ice surface, this assumption may be shown as consistent with the thin water layer approximation used in the following section. All of the parameters in the above heat terms are defined in the Nomenclature section. Further information on energy sources in a freezing system may be found in [2, 3].

In aircraft icing codes, the icing calculation represents only one part of the problem. It is also necessary to calculate the air flow and droplet trajectories; the method is detailed in [3]. Of interest to the present study is the fact that during an ice growth calculation a control volume is constructed, with an upper limit which coincides with the boundary layer of the air flow and a lower limit below the ice surface. Hence all of the above parameter values are known, having being determined in the boundary layer calculation. Clearly, as the ice grows the boundary layer must be recalculated and so the parameters are in fact time dependent. Taking constant parameter values could be viewed as dealing with only a single step of a multi-timestep calculation and the values would subsequently be adjusted to new constants for the following timestep. In reality, most codes are only used for one step calculations, where all the parameters are determined from the flow over a clean aerofoil. Hence, in the present study, to be consistent with icing codes and for simplicity, the parameter values are constant.

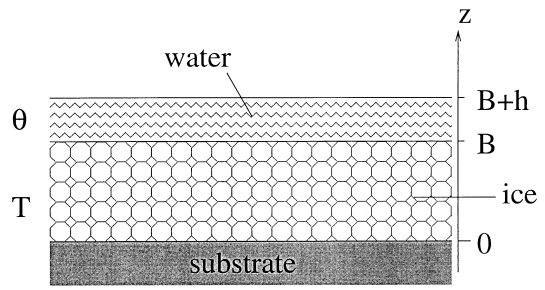

Fig. 1. Schematic of the system.

Balancing all the energy terms leads to

$$Q_c + Q_e + Q_d = Q_k + Q_l + Q_a + Q_f.$$

From this heat balance an estimate for the freezing fraction (the mass fraction of water which will turn to ice as it encounters the aircraft surface) can be obtained by setting the temperature in the ice and water layers to zero. If this returns a freezing fraction greater than 1, then only rime ice will occur. Setting the freezing fraction to one then allows an average temperature to be obtained. Similarly, if the freezing fraction is found to be less than zero, then it is taken as identically zero and the (above zero) average temperature estimated. A value between 0 and 1 is taken as correct and used in subsequent calculations for glaze ice growth, with the average temperature held at zero degrees.

Whilst this method has been used for a number of years to predict aircraft ice growth, a more rigorous formulation should provide significantly more information. In particular, solving the heat equations in the ice and water will improve the heat transfer estimates. The mathematical approach will also provide more information about freezing rates, which in turn relate to the strength of the ice.

2.2. The Stefan problem

A more rigorous mathematical approach to modelling ice growth is to specify a Stefan problem. These are used extensively in the investigation of melting or solidification. Mathematically equivalent problems arise in the study of diffusion and chemical reactions, see [6, 10]. The heat balance terms of the previous section then appear as boundary conditions to the governing equations.

In the following analysis only the one-dimensional model will be considered. The configuration is depicted in Fig. 1, which shows ice and water layers of thickness $B(t)$ and $h(t)$, respectively. The temperature in the ice is denoted by $T(z, t)$, whilst in the water layer it is denoted $\theta(z, t)$. The relevant heat equations are then

$$\frac{\partial T}{\partial t} = \frac{\kappa_i\, \partial^2 T}{\rho_i c_i\, \partial z^2} \tag{1}$$

$$\frac{\partial \theta}{\partial t} = \frac{\kappa_w\, \partial^2 \theta}{\rho_w c_w\, \partial z^2} \tag{2}$$

where κ, ρ and c are the thermal conductivity, density and specific heat, subscripts i and w denote ice and water.

At the moving ice/water interface, $B(t)$, there is a Stefan condition:

$$\rho_i L\frac{\partial B}{\partial t} = \kappa_i\frac{\partial T}{\partial z} - \kappa_w\frac{\partial \theta}{\partial z} \tag{3}$$

which states that the velocity of the interface is proportional to the heat flux across it; L is the latent heat of fusion, see [10]. A mass balance gives a relation between the ice and water height and the incoming fluid:

$$\rho_i\frac{\partial B}{\partial t} + \rho_w\frac{\partial h}{\partial t} = \beta WG. \tag{4}$$

To conform with the aircraft literature, the amount of incoming fluid is here written as the product of the collection efficiency, free stream velocity and the liquid water content of the air, rather than as a single quantity.

Provided there exists an ice layer with water on top (subsequent analysis shows that this is not always the case), this system of equations requires solving subject to the following boundary conditions. At the free surface, $z = B(t)+h(t)$, a cooling condition is applied, stating that the heat flux across the free surface is determined by convection, heat from the incoming droplets, evaporation, aerodynamic heating and kinetic energy

$$\kappa_w\frac{\partial \theta}{\partial z} = \bar{H}_{aw}(\theta(B+h,t)-T_a)+\beta WGc_w(\theta(B+h,t)-T_a)$$

$$+\chi[e(\theta(B+h,t))-e(T_a))]-\frac{r\bar{H}_{aw}W^2}{2c_a}-\frac{(\beta WG)W^2}{2}. \tag{5}$$

In the following work the term in square brackets will be approximated by a linear relation, $e(\theta)-e(T_a)\approx e_0(\theta-T_a)$. This will clearly be a reasonable assumption over a small enough temperature range. Using data from [15], the constant e_0 is taken as 44.4 in [8], for a temperature variation of a few degrees. This simple approximation will here be assumed to hold over a wider range, $T\in[-15,0]^\circ$C. The evaporation coefficient, χ, is described in [1, 2].

At the freezing front, $z = B(t)$, the ice and water are at the freezing temperature:

$$T(B,t) = T_f = \theta(B,t). \tag{6}$$

For generality, T_f will be left unspecified in the following analysis, however in the results section it is taken to be 0°C. The air and substrate temperatures will be assumed to be sub-zero. In the present study two different boundary conditions have been used; either a cooling condition or fixed temperature:

$$\kappa_i\left.\frac{\partial T}{\partial z}\right|_{z=0} = \bar{H}_{is}(T(0,t)-T_s) \qquad T(0,t) = T_s. \tag{7}$$

Assuming an initially clean substrate, the appropriate initial conditions are

$$B(0) = 0 = h(0). \tag{8}$$

The system of Eqs. (1)–(4) together with the boundary and initial conditions (5)–(8) are sufficient to fully determine the temperature throughout the ice and water and to calculate the thickness of each layer. In the semi-infinite media, the simplified problem of freezing with the substrate temperature fixed to T_f, may be solved analytically in terms of the error function, see, for example, [16, Chap. 11]. In the present case, with only a finite layer of water, no known analytic solution exists.

3. Thin film approximations

3.1. Fixed temperature substrate

With the temperature fixed below freezing at the substrate, the freezing process occurs in two distinct stages. During the first stage, all of the incoming water freezes almost instantaneously, whilst in the second stage, both water and ice develop simultaneously. The physical reason for this two stage process is that the model effectively specifies an infinite heat transfer coefficient at the substrate. The initial incoming water must therefore immediately adopt the sub-zero substrate temperature and, since there is now a nucleation site, freeze. Only when there is a sufficiently thick insulating layer and enough energy has been introduced into the system can water appear.

During the first stage, when only ice is growing, the thickness of the ice is found by integrating the mass balance (4), with the water thickness term set to zero, to give

$$B = \frac{\beta WG}{\rho_i}t. \tag{9}$$

Non-dimensionalising the heat equation for the ice (1), with the time-scale taken from (9) leads to

$$\frac{\partial^2 T'}{\partial z'^2} = \frac{\beta WGc_i\hat{B}\partial T'}{\kappa_i\quad\partial t'} = \varepsilon\frac{\partial T'}{\partial t'} \tag{10}$$

where $\hat{B}$ is the height-scale and primes denote non-dimensional quantities. The right hand side of (10) will be negligible, to leading order, provided $\varepsilon\ll 1$, that is, if the height-scale satisfies

$$\hat{B} \ll \frac{\kappa_i}{\beta WGc_i}.$$

Taking typical values for the constants given in Table 1 indicates $\kappa_i/\beta WGc_i = 2.4$ cm. If the ice thickness does satisfy this relation, the leading-order problem becomes, in dimensional form,

$$\frac{\partial^2 T}{\partial z^2} = 0. \tag{11}$$

The ice temperature profile may then be calculated by integrating (11) subject to (7b) and a form for the cooling condition appropriate to ice

Table 1
Parameter values used for Figs 2–5

c_a	1014	J kg^{-1} K^{-1}	L	3.344×10^5	J kg^{-1}
c_i	2030	J kg^{-1} K^{-1}	L_E	2.5×10^6	J kg^{-1}
c_w	4220	J kg^{-1} K^{-1}	p_0	9×10^4	Pa
e_0	44.4	Pa K^{-1}	W	90	m s^{-1}
G	0.001	kg m^{-3}	r	0.875	
$\bar{H}_{aw}$	500	W m^{-2} K^{-1}	β	0.5	
$\bar{H}_{is}$	1000	W m^{-2} K^{-1}	ρ_i	917	kg m^{-3}
κ_i	2.18	W m^{-1} K^{-1}	ρ_w	1000	kg m^{-3}
κ_w	0.571	W m^{-1} K^{-1}	χ	8.52	m s^{-1}
l_e	0.875				

$$-\kappa_i\frac{\partial T}{\partial z} = (\bar{H}_{ai}+\beta WGc_w+\chi_s e_0)(T(B,t)-T_a) - \frac{r\bar{H}_{ai}W^2}{2c_a}-\frac{(\beta WG)W^2}{2}. \quad (12)$$

Eq. (11) indicates that the temperature profile is linear in z, but not in t. This type of problem is termed quasi or pseudo-steady, since time only enters through the moving boundary conditions, applied at $z = B(t)$. The physical interpretation of this approximately linear z dependence is that the time-scale for ice growth, determined by the amount of incoming fluid, is much slower than that for conduction through the ice. So the temperature has time to equilibrate as the ice slowly accumulates. Quasi-steady problems typically arise when the region of interest is 'thin', examples may be found in numerous physical situations including reaction–diffusion systems [11, Chap. 5] or viscous flow [13, 14]. They are a particular example of a singular perturbation, see [12] for example, since neglecting the time derivative means that the solution becomes invalid as $t\to0$ and the initial condition will not be satisfied. This singular limit is not considered in the current analysis.

In the second stage, a water layer develops on top of the ice. Again the heat equations may be simplified, via a similar argument to that of the preceding section, to quasi-steady forms

$$\frac{\partial^2 T}{\partial x^2}\approx 0 \qquad \frac{\partial^2\theta}{\partial z^2}\approx 0 \quad (13)$$

provided

$$\hat{B}\ll\frac{\kappa_i}{(1-\phi)\beta WGc_i}\sim\frac{0.02}{1-\phi}\ \text{m}$$

$$\hat{h}\ll\frac{\kappa_w}{\phi\beta WGc_w}\sim\frac{0.003}{\phi}\ \text{m}.$$

Here, ϕ is the fraction of water which remains liquid, so the argument leading to (11) is strengthened, with 2 cm being a conservative estimate. The water layer, however, must remain thin (unless there is a slow build-up of water, $\phi\ll1$, which allows time for the temperature to adjust), with 3 mm being the lower value of the estimate. This is well within the limit of water thickness expected in aircraft icing conditions.

If the water and ice layers do satisfy the above inequalities, the temperature in the ice is

$$T=\frac{T_f-T_s}{B}z+T_s, \quad (14)$$

where (6) and (7b) have been imposed. The temperature in the water is obtained by integrating (13) subject to (5) and (6):

$$\theta=\frac{a_0-a_1(T_f-T_a)}{1+a_1h}(z-B)+T_f \quad (15)$$

where

$$a_0=\frac{r\bar{H}_{aw}W^2}{2c_a\kappa_w}+\frac{\beta W^3G}{2\kappa_w}$$

$$a_1=\frac{\bar{H}_{aw}+\beta WGc_w+\chi e_0}{\kappa_w}. \quad (16)$$

The constant a_0 represents the energy sources due to droplet kinetic energy and aerodynamic heating. The energy sinks, due to convective heat loss, cooling by incoming droplets and evaporation are contained in a_1.

Up until this stage, the analysis has closely followed the work of [2], which concerns icing on power cables. The main difference coming from the inclusion of certain energy terms, appropriate for a fast moving system, such as aerodynamic heating and droplet kinetic energy. Now a qualitative difference has appeared, in the form of the denominator in (15). In [2] the term a_1h is neglected. This simplification may be achieved by taking the leading order term in the Taylor series expansion of the right hand side of Eq. (5), with h as the small parameter. However, in general, the water occupies a thin layer so the temperature gradient will be large (in fact of the order $\Delta\theta/h$, where $\Delta\theta$ is the temperature difference across the layer) and so the series is invalid for temperature variations $\Delta\theta\sim O(1)$. An a priori calculation of typical

values for $a_1 h$ do indeed show it to be $O(1)$ and so forms an intrinsic part of the system.

Substituting for the temperature in the Stefan condition leads to

$$\frac{\partial B}{\partial t} = \frac{a_2}{B} - \frac{a_3}{1+a_1 h} \tag{17}$$

where

$$a_2 = \frac{\kappa_i (T_f - T_s)}{\rho_i L}$$

$$a_3 = \frac{\kappa_w (a_0 - a_1 (T_f - T_a))}{\rho_i L}. \tag{18}$$

Conduction through the ice is specified by the first term on the right hand side of (17). This shows that the ice growth rate increases with decreasing substrate temperature and decreasing ice thickness. The second term on the right hand side of (17) is proportional to a_3, which incorporates the energy source and sink terms a_0 and a_1. This indicates that as the energy sources increase the ice growth rate decreases. The energy sink terms have the opposite effect; increasing the energy sinks increases the growth rate. The thickness of the water layer also plays a role, demonstrated in the denominator of this final term. If $a_3 > 0$ (the energy source terms dominate) then this final term always acts to decrease the ice thickness. This effect will diminish as h increases and the water layer insulates the ice from the surface heating. If $a_3 < 0$ (energy sink terms dominate) the final term acts to enhance the ice growth, decreasing h increases the rate at which the cooling effects reach the ice/water interface and so speeds up the growth.

As $h \to 0$, $a_1 h$ becomes negligible and the ice growth rate is not affected by the water layer thickness. The problem then becomes equivalent to one where the water surface is linearised onto the ice surface and the boundary conditions at $z = B + h$ may be applied at $z = B$, as in the analysis of [2]. The governing equation for the ice thickness in this case is separable and may be integrated immediately. However, in the current general case, Eq. (17) must be solved numerically.

Integrating the mass balance provides another relation between the ice and water thickness

$$\rho_i (B - B_w) + \rho_w h = \beta W G (t - t_w) \tag{19}$$

where B_w is the ice thickness where water first appears, at time t_w. These are related by

$$B_w = \frac{\beta W G}{\rho_i} t_w. \tag{20}$$

To determine B_w a continuity argument is used. In the limit $h \to 0$, the ice thickness, given by (17) must match that predicted by (9), so

$$\frac{\beta W G}{\rho_i} = \frac{a_1}{B_w} - a_3 \tag{21}$$

and

$$B_w = \frac{a_2 \rho_i}{\rho_i a_3 + \beta W G}. \tag{22}$$

The factors affecting the rime ice thickness are now evident from Eq. (22). B_w is proportional to a_2, the ice conduction term, so decreasing the substrate temperature increases the rime ice thickness. Increasing the energy source terms contained in a_3 or the rate at which fluid impinges will decrease B_w. Increasing the energy sink terms in a_3 will have the opposite effect.

The two stage calculation, to determine the ice and water growth, with a fixed temperature substrate, can now be fully specified. First, apply (9) until time $t = t_w$ ($= \rho_i B_w / \beta W G$). The rime ice calculation is then complete. Next, numerically solve Eq. (17), with h determined from (19), to determine the glaze ice growth. Finally, the ice thickness can be substituted back into (19) to determine the water layer thickness.

3.2. Cooling condition at the substrate

In the previous section the ice and substrate have been treated as a composite media, that is, one with an intimate contact at the interface. Further, the assumption of a constant, prescribed substrate temperature indicates the substrate has a large thermal mass and a conductivity much higher than that of the ice. A less intimate contact requires a cooling condition to be applied at the interface. This is discussed in the current section where, again, the substrate temperature will be a prescribed constant. The results of the previous section may be retrieved by allowing the heat transfer coefficient between the ice and substrate to tend to infinity.

With this new form for the boundary condition at the ice/substrate interface, qualitatively different results may be obtained. In particular, for a sufficiently low value, ice and water may grow together for all time. It is also possible for only water to appear initially. So, at time $t = 0$ there are three possible scenarios. Assuming ice and water grow together for all time, the temperature in the ice is

$$T = \frac{\bar{H}_{is} (T_f - T_s)}{\kappa_i + \bar{H}_{is} B} z + \frac{\kappa_i T_f + \bar{H}_{is} T_s B}{\kappa_i + \bar{H}_{is} B} \tag{23}$$

whilst (15) still holds in the water. The Stefan condition then reduces to

$$\frac{\partial B}{\partial t} = \frac{a_2}{a_4 + B} - \frac{a_3}{1 + a_1 h} \tag{24}$$

where

$$a_4 = \frac{\kappa_i}{\bar{H}_{is}}. \tag{25}$$

The physical mechanisms driving (24) are the same as in the previous section, except now the heat transfer into the substrate is incorporated, with the inclusion of the term a_4. The three possibilities are recognised by cal-

culating the initial values for ice and water growth rates from (24) and (4):

1. Initial ice growth

$$\frac{\partial B}{\partial t}>0 \quad \frac{\partial h}{\partial t}>0$$

2. Initial ice and water growth

$$\frac{\partial B}{\partial t}>0 \quad \frac{\partial h}{\partial t}>0$$

3. Initial water growth

$$\frac{\partial B}{\partial t}<0 \quad \frac{\partial h}{\partial t}>0$$

In case (1), the model follows that of the previous section, with only ice growing until time t_w. Now, the ice thickness at which water appears is

$$B_w=\frac{a_2\rho_i}{a_3\rho_i+\beta WG}-a_4. \tag{26}$$

As $\bar{H}_{is}\to\infty$, this reduces to the value given by (22). In case (2) the calculations are again identical, but with B_w and t_w set to zero. Case (3) requires the water temperature to be recalculated, subject to cooling conditions at both the air and substrate (at the substrate this requires using (7a) with $\bar{H}_{is}$ and T replaced with $\bar{H}_{ws}$ and θ). The water temperature is now

$$\theta=A_1z+A_0 \tag{27}$$

where

$$A_0=\frac{a_5(a_0+a_1T_a)+T_s(1+a_1h)}{1+a_1(h+a_5)},$$

$$A_1=\frac{A_0-T_s}{a_5},$$

$$a_5=\frac{\kappa_w}{H_{ws}}. \tag{28}$$

Ice will only form when the water temperature reaches T_f. Imposing this value of θ in (27) allows the water thickness at which ice first appears, h_w, to be determined. The corresponding time is

$$t_w=\frac{\rho_w}{\beta WG}h_w \tag{29}$$

The ice calculation then proceeds as normal, by integrating (24), subject to $B(t_w)=0$, $h(t_w)=h_w$.

4. Results

The parameter values for this and the following examples are given in Table 1. Fig. 2 shows the growth of ice and water over a period of 100 s, for relatively warm conditions when the air and substrate temperatures $T_a=T_s=-1°C$. the curves labelled (T) are ice and the sum of ice and water thicknesses for the fixed substrate temperature model. Those labelled (C) correspond to the

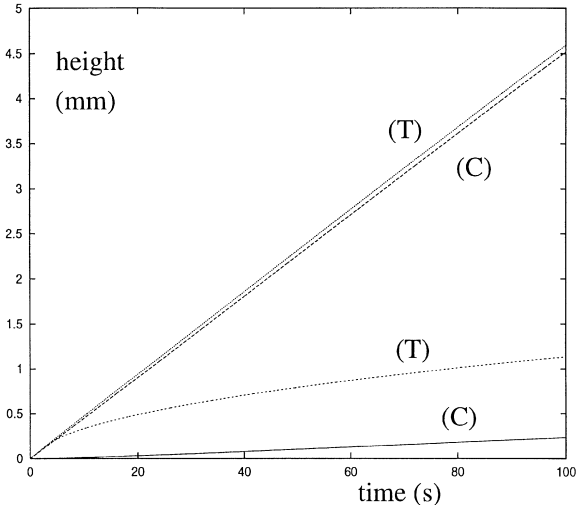

Fig. 2. Ice and water growth for $T_a=-1$, $T_s=-1°C$.

cooling condition at the substrate. In this case, the (T) curves show only ice growing for the first 2.8 s, after which most of the incoming water remains unfrozen. In contrast to this, the (C) curve is an example of type 2), where ice and water grow simultaneously for all time. Note, since water is more dense than ice, the (C) water curve lies slightly below the (T) curve.

The large difference between the two sets of curves is due to the choice of heat transfer coefficient $\bar{H}_{is}$. The value of 1000 W m^{-2} K^{-1} was chosen arbitrarily to highlight the qualitative differences between the two models. Increasing this value would cause the curves to come closer together and coincide as $\bar{H}_{is}\to\infty$. Since this choice has no relation to experimental results, in the following discussion of experimental observations, only the results for a fixed substrate temperature will be used for comparison.

Reducing the substrate temperature to $-10°C$ leads to the results shown in Fig. 3. Eqs. (22) and (26) demonstrate that the rime ice thickness is proportional to the substrate temperature (since $T_f=0$), hence the (T) curves show a much greater accumulation of ice than in the previous example. Since the time for rime growth is proportional to the thickness, t_w is correspondingly greater than in the previous example, $t_w=27.9$ s. The (C) curves again show type 2) behaviour.

Increasing the substrate temperature and decreasing the air temperature, $T_a=-10$, $T_s=-1°C$, leads to the results shown in Fig. 4. In this case the ice layer is considerably thinner than in the previous one, indicating the relative importance of the substrate and air temperature. Although the discussion leading to Eq. (31) indicates that under certain circumstances the air temperature can be much more important than the substrate temperature, provided $T_s<0$.

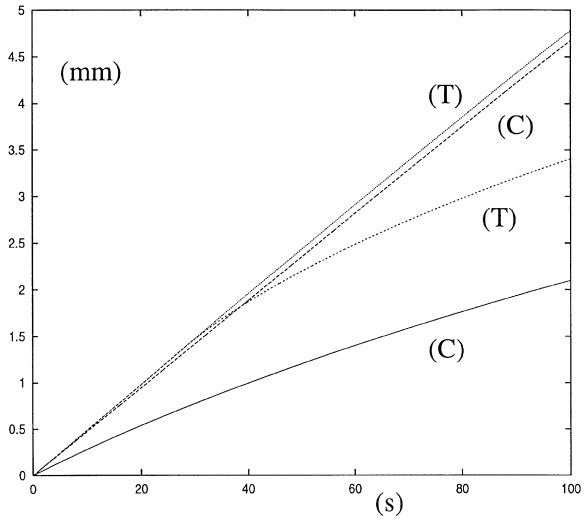

Fig. 3. Ice and water growth for $T_a = -1$, $T_s = -10$°C.

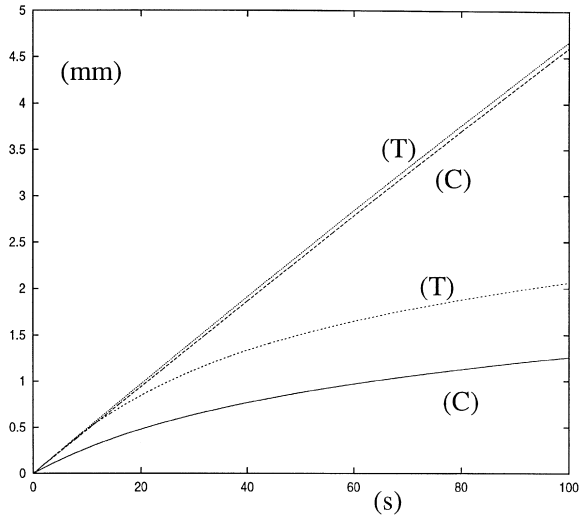

Fig. 4. Ice and water growth for $T_a = -10$, $T_s = -1$°C.

Fig. 5 shows results for $T_a = -10$, $T_s = -10$°C. As expected, this leads to the most rapid ice growth. On the (T) curves, water only starts to appear after $t_w = 69.9$ s, after which time the majority of incoming liquid turns to ice. The ice thickness when water first appears is 3.43 mm. The (C) curves show water appearing after 25.5 s.

As an illustration of the practical element of this work, Fig. 6 shows a thin section of a piece of ice grown in an icing wind tunnel. The microstructure is highlighted by the use of a strong background light source, which may be partially seen to the right of the ice section. The accretion was formed in approximately 12 min on a NACA 0012 aluminium model. This is a standard two-dimensional leading edge shape, which in this case has

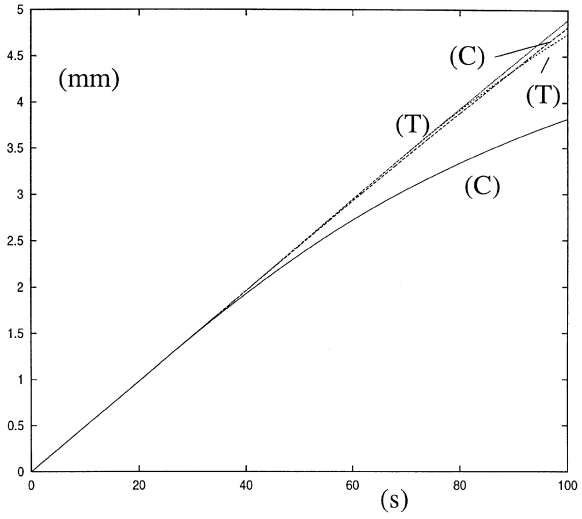

Fig. 5. Ice and water growth for $T_a = -10$, $T_s = -10$°C.

dimensions of 40 cm × 4.8 cm, hence the curvature is considerably greater than that on an aircraft wing. The ambient freestream and initial substrate temperature was approximately −10°C, the freestream velocity was 90 m s^{-1} and the liquid water concentration was 0.1 g m^{-3}. The ice grew from right to left, into the air flow. Whilst some of the specimen has been broken away during the process of recovering it, a layer of fine columnar grains (associated with rime ice growth—no water present) can be seen near the original growth front. As the accretion has continued to grow, the grain structure has become coarser (associated with glaze ice growth). It is encouraging to note that the depth of the fine grained region is approximately 2–3 mm which is in keeping with the model prediction for rime ice thickness in the case of the fixed substrate temperature model, for these approximate conditions.

Another point of interest is that both (22) and (26) permit a singularity, indicating that, for certain conditions the ice thickness at which water first appears, B_w, may become infinite. This is in keeping with experimental work, where water does not always appear. To understand this, consider the value given by (22)

$$B_w = \frac{\kappa_i(T_f - T_s)}{\kappa_w(a_0 - a_1(T_f - T_a)) + \beta WGL}. \tag{30}$$

Provided the substrate temperature is sub-zero and $T_f = 0$, the numerator is positive. Taking the parameter values given in Table 1, to determine a_0 and a_1, the denominator is also positive for $T_a = T_f$ and so a finite, positive value is obtained for B_w. Decreasing T_a increases the value of B_w until a value is reached where the denominator is zero:

$$T_a = T_f - \frac{1}{a_1}\left(\frac{\beta WGL}{\kappa_w} + a_0\right) \approx -15.98. \tag{31}$$

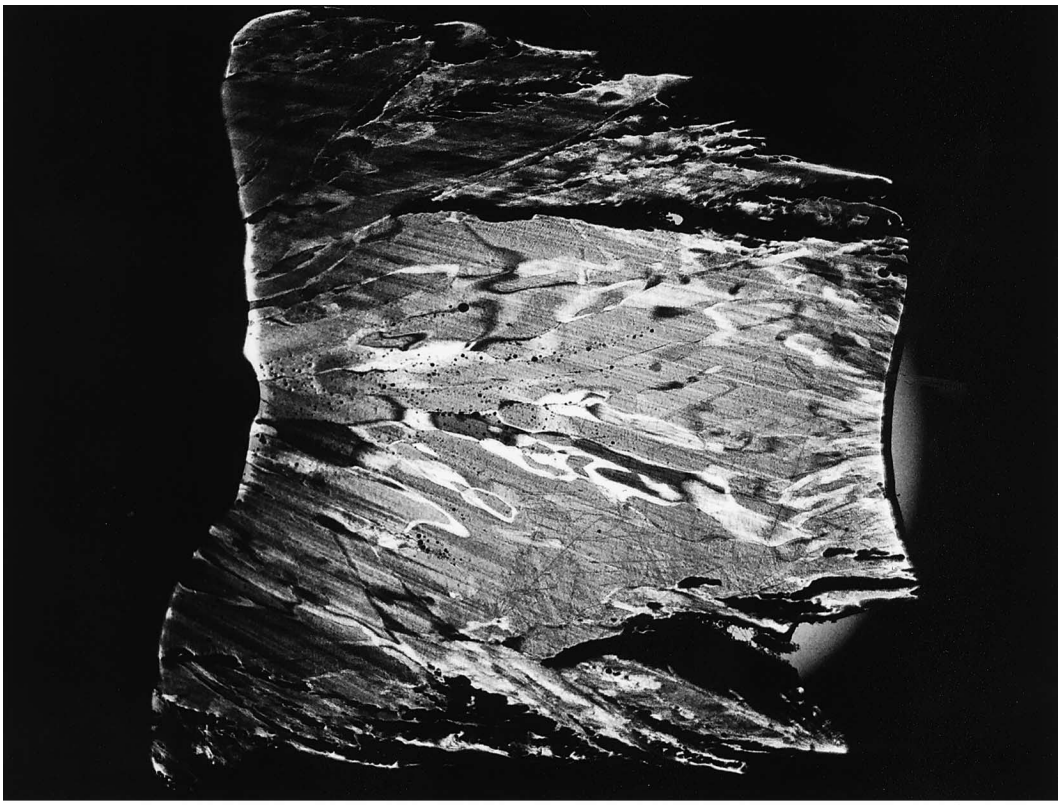

Fig. 6. Microstructure of a piece of ice grown on a model aluminium aerofoil (NACA 0012) at -10°C.

This temperature is of the correct magnitude when compared to experimental evidence on the glaze/time temperature threshold, although slightly high. However, due to the nature of the singularity it is likely that a lower value would be observed in practice. Taking $T_a = -15.5^{\circ}$C, leads to water first appearing when the ice is 4 cm thick; most ice accretion experiments would have been terminated well before this. Further, the subsequent water layer will remain thin for some time and is therefore less likely to be detected. Air temperatures below this critical value will have a negative B_w, according to the present theory. This signifies that the model assumptions have become invalid, since the ice temperature never becomes high enough for water to appear. Hence, the basis of the model, that ice and water grow simultaneously is not satisfied. The mass balance (9) is then sufficient to fully determine the ice thickness.

5. Conclusion

A mathematical model has been developed to determine ice and water growth in the presence of incoming supercooled droplets. The leading order problem, for relatively thin layers, reduces to a single first order differential equation for the ice thickness, which requires solving numerically, Once this has been achieved, quantities such as the water thickness and temperature profiles can be readily calculated.

With a fixed temperature at the substrate, the results show that only ice will grow initially. This occurs since the substrate provides many nucleation points and so, since the initial water droplets must adopt the sub-zero substrate temperature, freezing takes place. Subsequently, provided conditions are sufficiently mild, a water layer will appear. It is encouraging that the microstructural observations of Fig. 6 appear to reflect this transition from dry to wet ice growth.

The relative effect of the driving mechanisms behind the ice growth can be easily identified from this analysis. In particular, with a fixed substrate temperature, the rime ice thickness increases:

- proportional to the temperature difference between freezing and the substrate, $T_f - F_s$.
- decreasing a_3, which decreases with decreasing energy source terms or growing energy sink terms

- with decreasing incoming fluid.

Eq. (22) allows the conditions to be determined where rime ice never forms, $B_w \to 0$, or glaze ice never forms, $B_w \to \infty$. Experimental evidence confirms the validity of Eq. (22). When glaze ice does occur, the ice growth rate increases with

- increasing $a_2 \propto T_f - T_s$
- decreasing a_3
- increasing the water layer thickness, h, when $a_3 > 0$ (the energy source terms dominate) or decreasing h when $a_3 < 0$ (the energy sink terms dominate).

A cooling condition at the substrate, depending on the heat transfer coefficient there, can either lead to initial pure ice growth, simultaneous ice and water growth or pure water growth. Again the present model may be used to estimate the conditions at which rime ice or water never appear, via Eq. (26). The factors affecting glaze ice growth, shown in Eq. (24), are the same as those described above for the fixed temperature substrate, with the added condition that increasing the heat transfer between the ice and the (sub-zero) substrate increases the ice growth rate.

By tackling this physical situation using a Stefan model, the present method can provide information on temperature distributions and freezing rates. The freezing rate, in particular, is a useful descriptor of local ice forming conditions and has a direct bearing on the grain size, which may be measured directly. The grain structure in turn determines the ice strength. This type of model therefore provides significantly more information than does the energy balance method currently employed in icing codes.

Acknowledgements

We would like to thank Mr R.W. Gent of DERA (Defence Evaluation and Research Agency) and Dr A.C. Fowler of Oxford University for helpful comments during the preparation of this manuscript.

The ICECREMO project (The Development of three-dimensional Ice Accretion Modelling) is a collaboration between British Aerospace, Rolls–Royce, Westland Helicopters and DERA. The project is managed by the British Aerospace and is part funded by the DTI under Contract RA/6/31/05.

References

[1] T.J. Chilton, A.P. Colburn, Mass transfer (absorption) coefficients, Ind. Eng. Chem. 26 (1934) 1183–1187.
[2] G.I. Poots, in: Ice and snow accretion on structures, Res. Stud. Press, 1996.
[3] S.K. Thomas, R.P. Cassoni, C.D. MacArthur, Aircraft anti-icing and de-icing techniques and modelling, J. Aircraft 33 (5) (1996) 841–854.
[4] T.G. Myers, C.P. Thompson, Modelling the flow of water on aircraft in icing conditions, AIAA J. 36 (6) (1998) 1010–1013.
[5] T.G. Myers, C.P. Thompson, V.K.S.S. Bandakhavai, Modelling water flow on aircraft in icing conditions. Part I: theory and results, in: 15th IMACS World Congress, vol. 5 Systems Engineering, Wissenschaft and Technik Verlag, Berlin, 1997, pp. 643–648.
[6] J.D. Crank, in: Free and Moving Boundary Value Problems, Oxford Science Publications, 1984.
[7] J.R. Lister, The solidification of buoyancy-driven flow in a flexible-walled channel, Parts I and II, JFM 272 (1994) 21–65.
[8] G.I. Poots, P.L.I. Skelton, Rime- and glaze-ice accretion due to freezing rain falling vertically on a horizontal thermally insulated overhead line conductor, Int. J. Heat Fl. Flow 13 (4) (1992) 390–398.
[9] B.L. Messinger, Equilibrium temperature of an unheated icing surface as a function of air speed, J. Aero. Sci. (1953) 29–42.
[10] J.M. Hill, in: One-dimensional Stefan Problems: An Introduction, Longman Sc. Tech. Press, 1987.
[11] J.D. Murray, in: Mathematical Biology, Springer-Verlag, Heidelberg, 1989.
[12] J.D. Murray, in: Applied Mathematical Sciences, Vol. 48, Asymptotic Analysis, Springer-Verlag, New York, 1984.
[13] H.P. Greenspan, On the motion of a small viscous droplet that wets a surface, JFM 84 (1978) 125–143.
[14] J.A. Moriarty, L.W. Schwartz, E.O. Tuck, Unsteady spreading of thin liquid films with small surface tension, Phys. Fl. A3 (5) (1991) 733–742.
[15] P.R. Lowe, An approximating polynomial for the computation of saturation pressure, J. Appl. Meteor. 16 (1977) 100–103.
[16] H.S. Carslaw, J.C. Jaeger, in: Conduction of Heat in Solids, Clarendon Press, Oxford, 1959.